LBL-7294
UC-37

NOISE CONSIDERATIONS IN MILLIMETER-WAVE SPECTROMETERS

W. D. Zoellner, W. F. Kolbe, B. Leskovar

December 1978

Prepared for the U. S. Department of Energy
under Contract W-7405-ENG-48

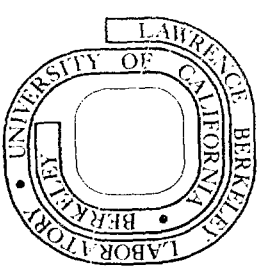

NOISE CONSIDERATIONS IN MILLIMETER-WAVE SPECTROMETERS

W. D. Zoellner, W. F. Kolbe, B. Leskovar
Lawrence Berkeley Laboratory
University of California
Berkeley, California 94720, U.S.A.

December 15, 1978

Abstract

An improved version of a microwave spectrometer operating in the vicinity of 70 GHz is described. The spectrometer, which incorporates a Fabry-Perot resonator and superheterodyne detection for high sensitivity is designed for the detection of gaseous pollutants and other atmospheric constituents. The instrument is capable of detecting polar molecules with absorption coefficients as small as $2 \times 10^{-9} cm^{-1}$. For sulphur dioxide diluted in air, this sensitivity corresponds to a detection limit of 1.2 ppm without preconcentration and with a time constant of 1 second. Measurements and analysis of the noise contributions limiting the sensitivity are presented.

1. Introduction

In previous reports, (1,2), we described the construction of a new microwave spectrometer designed to measure the concentration of various pollutant gases and other atmospheric constituents. The spectrometer was designed around a high-Q Fabry-Perot resonator as a sample cell, and employed superheterodyne detection to obtain high sensitivity at low microwave power levels. The performance of the instrument was discussed and various sources of noise limiting the sensitivity were identified. Measurements were made of low concentrations of SO_2 gas employing the 6(1,5)-6(0,6) rotational transition (3) at a frequency of 68.972 GHz.

Since that time a more detailed analysis of the noise contributions has been made. A number of improvements in the spectrometer system have resulted, leading to greater sensitivity. In addition, the microwave resonator previously described, (1,4,5), has been replaced with a newly designed version having higher Q and improved mechanical properties. In this report, these improvements are described and interpreted in terms of the noise characteristics of the system.

In the next section (section 2) the basic components of the spectrometer, including the mechanical construction of the new resonator, are described. Section 3 deals with the influence of noise on the overall performance and explains the improvements resulting from the modifications of the previous spectrometer. Section 5 describes the performance of the system and points out the restrictions in the choice of operating parameters necessary to observe the gas absorption signal with maximum sensitivity. It shows as a practical result, measurements of the prototype gas, SO_2 at various concentrations.

2. Description of the Spectrometer System

A block diagram of the spectrometer is shown in Fig. 1. The system consists of the following major components: a signal oscillator, a local oscillator, a low-noise receiver, and the improved Fabry-Perot microwave cavity mounted in a vacuum enclosure. The frequency of the Gunn oscillator, which serves as the signal source, is doubled. This yields up to approximately 5 mW of microwave power in the vicinity of 70 GHz. The Gunn oscillator can be tuned electronically by means of a varactor diode.

The local oscillator is a klystron, which is phase-locked to the doubled frequency of the signal oscillator by means of a mixer and a stabilizer. Since the stabilizer uses a 30 MHz IF amplifier and phase detector, the local oscillator is always maintained at a constant phase and frequency off-set of 30 MHz

from the signal oscillator. The 30 MHz reference is derived from the master oscillator of a frequency synthesizer.

A semi-confocal Fabry-Perot transmission resonator is used as a sample cell. This type of resonator, which consists of a concave spherical mirror and an opposing flat mirror having two waveguide coupling ports, has the advantage of high sensitivity and easy tuneability.

For the present spectrometer, a new Fabry-Perot microwave resonator and vacuum enclosure was constructed. The completed cavity, shown in Fig. 2a and 2b is similar to a previous design (4,5) but incorporates a number of improvements. The vacuum chamber has been reduced in size to enclose only the actual cavity region itself. It is constructed of glass and plastic and is provided with teflon vacuum seals which permit the observation of unstable molecular species. A new microwave coupling structure has also been designed with reduced losses resulting in a higher Q. Finally, a stepping motor drive has been provided to permit large frequency sweeps under computer control. As before, fine electrical tuning is achieved by means of a piezoelectric transducer.

The microwave resonator itself consists of two opposing mirrors, one flat and one concave spherical. The mirrors are mounted in a semiconfocal configuration in which the radius of curvature of the spherical mirror is approximately twice the mirror spacing. This geometry has the advantage that it is noncritical in alignment, is compact, and exhibits a high Q. Resonances occur according to the relation (11).

$$\frac{4d}{\lambda} = 2q + 1/2, \quad q = 1, 2, 3, \ldots$$

where d is the mirror spacing, λ is the wavelength of the microwave radiation and q is the number of half-wavelengths between the mirrors.

The mirrors were constructed from beryllium-copper blanks 5.37 cm in diameter. The concave mirror has a radius of curvature of 14.86 cm. The mirrors were ground and polished to optical

tolerances and plated with approximately 75 μ of silver for high electrical surface conductivity and 2 μ of gold for corrosion protection. The mirrors are mounted with a separation of 7.4 cm.

In order to couple microwave energy in and out of the resonator, two small holes were provided near the center of the face of the flat mirror. The coupling structures were constructed by electroforming two cylindrical copper plugs around aluminum mandrels of the same dimensions as the wave guide (WR-15) and machining the plated ends to leave a thin wall through which the coupling hole was drilled. The plugs were then soldered into round holes in the flat mirror. The spacing between holes is 6.2 mm. After machining the front surface of the mirror, the aluminum mandrels were removed with a hot, concentrated sodium hydroxide solution. Mounting holes provided at the rear of the mirror permitted two standard waveguides to be attached using conventional flanges suitably modified for close spacing. Thin mylar windows were used to provide a vacuum seal.

As shown in Fig. 2a, the concave mirror is moveable and is supported by a shaft extending from the stepping motor drive. Additional support is provided by the plastic housing surrounding the mirror and by a teflon sliding seal. A cylindrical piezoelectric transducer provides control of the fine motion of the mirror.

The transducer (Clevite PZT-5H) is a hollow cylinder 3.8 cm in diameter and 3.8 cm long fitted with copper electrodes on the inner and outer cylindrical surfaces. A low vapor pressure epoxy was used to attach it between the mirror and support shaft using stainless steel mounting rings.

The two microwave coupling irises were carefully enlarged to obtain the desired transmission characteristics and quality factor. The final diameter chosen was 1.0 mm for each of the two coupling holes. The wall thickness behind each hole was 0.13 mm. The transmission loss was 24 dB and the loaded Q was 72000. The Q was later reduced to 67000 after coating the mirrors with a thin

layer of teflon which was applied to inhibit the decomposition of free radicals.

Fig. 3 shows the resonator tuning behavior as a function of the piezoelectric drive voltage. It is seen that a total tuning range of more than 6 MHz is attainable. This is more than adequate for sweeping through any gas resonance line and for thermal drift compensation of the cavity system. Larger sweeps can be obtained by operating the stepping motor. In the figure, two curves, corresponding to upwards and downwards sweeps, show a significant hysteresis which can be attributed to the transducer characteristics. Since the transducer was operated inside a feedback loop, this behavior did not present a problem. Figure 4 shows the dynamic behavior of the tuning system. Resonances at 4 and 8 kHz were due to the mechanical components of the system. Their effects were eliminated by an appropriate roll off of the feedback amplification system.

The microwave receiver consists of a mixer/preamplifier with a (SSB) noise figure of about 11 dB. This is followed by an IF amplifier. The in-phase and quadrature components of the cavity response function are detected by means of a phase shifter and divider and two phase detectors.

The in-phase component is used to detect the changes in transmitted power through the cavity resulting from the sample gas absorption. The quadrature component provides information about the difference between the signal frequency and resonance frequency. The direct and quadrature output signals are illustrated in Fig. 5.

The quadrature output signal, after appropriate amplification and filtering, is fed back to the Gunn diode signal oscillator via a varactor input. In this way, the signal oscillator is maintained at the same frequency as the cavity resonance.

A PDP 11/34 computer sets the actual operating frequency to that required for the gas under investigation by controlling a frequency synthesizer operating in the vicinity of 450 MHz. A harmonic mixer multiplies this frequency by 76 and compares it with the frequency of the signal oscillator. A frequency discriminator

operating at 30 MHz provides a voltage proportional to the difference. After amplification, this voltage is fed into the piezoelectric transducer of the microwave resonator, thereby tuning it to the appropriate frequency. Since the signal oscillator is already controlled by the cavity resonance frequency, the whole system is now operating at the appropriate frequency for detection of the gas.

This new stabilization system differs from the arrangement previously used (described in Ref. 1,2). In the previous system, the signal oscillator was phase locked directly to the frequency synthesizer and the quadrature output of the receiver was used to control the cavity resonance frequency. As will be discussed below, this new arrangement results in better system performance.

As in the previous spectrometer, the signal detection capability is enhanced by the use of frequency modulation followed by phase sensitive detection using a lock-in amplifier. The modulating voltage at 93 Hz frequency is combined with the frequency discriminator signal as shown in the block diagram, Fig. 1. As a result, the source and local oscillators and the resonance frequency of the resonator all undergo the same periodic frequency changes.

The varying attenuation caused by the gas is then detected by the lock-in amplifier. The detected signal is processed by the computer via an analog-to-digital converter and can be stored or displayed.

3. System Noise Characterization

The sensitivity of the spectrometer is determined by the noise contributions of the signal source, the microwave cavity, and the receiver.

The thermal noise of the gas in the cavity can be neglected compared to the receiver noise as the noise temperature of the receiver is much higher than room temperature. If the receiver

noise is dominant in a system, one can try to overcome it by increasing the source power provided there are no restrictions, as for instance, saturation of the gas.

As soon as the source noise becomes dominant, increasing source power results in an increase of the total noise by the same amount as the signal so that no improvement is obtained. As pointed out in (1,2), source noise was the limiting factor for the sensitivity of the previous spectrometer.

The effect of source noise has been discussed by Strandberg (6), and by Leskovar et al (7). Two contributions are responsible for the total noise reaching the microwave receiver. The first is AM noise which passes directly through the microwave cavity and the second is FM noise which is converted by the slope of the cavity response curve into AM noise before reaching the receiver. The latter contribution is dominant in our case. For a maximum reduction of this noise, the source frequency should essentially coincide with the resonance frequency as then the slope of the direct output will be zero, yielding a negligible FM-AM conversion.

To obtain quantitative information, measurements were made of the noise-to-carrier ratio at the direct output of the spectrometer. An HP model 302A wave analyzer was used to measure the noise density at various offset frequencies ranging from 33 Hz to 10 KHz. The carrier power was established by offsetting the LO frequency difference, normally 30 MHz, by approximately 1 KHz and measuring the power of the resulting 1 KHz beat frequency with the same wave analyzer. The ratio obtained was normalized to a 1 Hz bandwidth. The measurements were repeated for several different microwave power levels.

The results are shown in Table 1. In the table the values obtained by the previous scheme and the present configuration are compared. Also shown is the noise contribution resulting from the receiver alone, as measured by setting the signal oscillator power to zero, thereby eliminating the source noise contribution.

It can be seen that in the previous arrangement, the influence of the source noise is dominant at all power levels measured as the overall noise-to-carrier ratio is not reduced when the power is increased. With the present scheme however, for power levels of -15 dBm or less, the observed values are only slightly greater than the noise contributions of the receiver alone. The source noise becomes dominant again only at higher power levels. The source noise contribution in the new scheme is thus approximately -122 dBm, a significant improvement over the value of -101 dBm obtained previously.

In the previous spectrometer configuration (1,2) the resonator had to track the frequency of the source. Because the resonator frequency was determined by the motion of mechanical components, only a moderate gain could be employed in the feedback loop to avoid oscillation. In the new system the source oscillator tracks the resonator. This is accomplished by feeding the correction voltage into the varactor input of the Gunn oscillator. As now no mechanical components are involved, the loop gain and bandwidth can be increased significantly. The reduction in source noise reported above is a direct result of this improvement.

In order to obtain further information about the nature of the source noise contribution, measurements of the noise-to-carrier ratio were made for the quadrature output signal. The same apparatus and measurements technique described above was used. Since the above measurements indicate significant source noise contributions only for the higher power levels, a value of -5 dBm was chosen for all the quadrature noise measurements. Data was obtained for offset frequencies extending from 33 Hz to 50 KHz and, as before, was normalized to a 1 Hz bandwidth.

The results are shown in Fig. 6. In curve (a) is shown the noise-to-carrier ratio obtained with the source oscillator tracking the Fabry-Perot resonator. This configuration thus corresponds to that used in normal operation of the spectrometer in its improved form. As can be seen, the noise amplitude is approximately independent of frequency, increasing by about 6 dB at the highest

frequency measured. The noise level is about 20 dB larger than that obtained at the direct output, reflecting the increased sensitivity of the quadrature signal to FM noise.

In curve (b) the feedback amplifier locking the source oscillator to the resonator has been turned off and the resonator has been carefully tuned to correspond to the source oscillator frequency. The Gunn diode source oscillator is now free running and as before, the local oscillator is phase-locked to it. The increased noise is a result of the frequency jitter (FM noise) of the free-running source as detected by the resonator response characteristic.

In order to separate the contribution of the resonator to the source noise conversion process from that of other components, it was removed from the system. A non-dispersive attenuator having a similar transmission loss was substituted and the noise measurements were repeated. The results are shown in curve (c) of the figure. Since the dispersive element has been removed, the noise signal is due to residual phase jitter between the signal oscillator and the local oscillator.

Curve (d) shows the background noise residual due to the receiver, obtained when the source power is reduced to zero. As can be seen, this noise is considerably smaller than the other noise contributions and can be neglected.

The conversion of a signal source contaminated by FM noise and passing through a transmission cavity has been given by Strandberg (6). Adapting Strandberg's results, which were derived for a "critically" coupled resonator, to the case of a resonator with a voltage transmission loss T_o, loaded quality factor Q_L and resonance frequency, ν_o we find for the phase detector

$$P_n(f) = 2BGL(f)P_oT_o^2(K_{quad}\sin^2\xi + K_{dir}\cos^2\xi) \qquad (1)$$

where

$$K_{quad} = 1 + 4Q_L^2f^2/\nu_o^2$$

$$K_{dir} = 4Q_L^2S^2(1 + 16Q_L^2f^2/\nu_o^2)$$

In this equation the quantity L(f) is the single sideband FM noise power density in a 1 Hz bandwidth, B is the actual bandwidth of the system, G is the gain of the receiver and phase detector, and P_o is the microwave power at the input of the cavity. f is the frequency offset from the carrier frequency, ν at which the noise is measured. $S = (\nu - \nu_o)/\nu_o$ is the normalized long term frequency deviation between the source oscillator frequency and the cavity resonance frequency.

In the derivation of Eq. (1) the assumption is made that the signal is phase detected against a noise free carrier with a phase angle ξ. If the angle $\xi = 0$, the direct output signal (proportional to K_{dir}) is detected and if $\xi = \pi/2$, the quadrature signal (proportional to K_{quad}) is obtained.

It can be shown that the first terms in both K_{quad} and K_{dir} (the quantity 1) are due to the frequency jitter between the reference carrier and the noise source, and the remaining terms (i.e. those containing Q_L) are due to the FM-AM conversion resulting from the resonator transfer function. In the present spectrometer, the local oscillator, which serves as the reference carrier, is phase locked to the signal oscillator. Thus the frequency jitter is significantly reduced and the first terms above should be replaced by $|1 - H(j2\pi f)|^2$ where $H(j2\pi f)$ is the transfer function of the phase lock loop (8,9).

If we note that the rms signal power, P_s is given by

$$P_s = \tfrac{1}{2} G P_o T_o^2$$

we can write for the quadrature output noise-to-carrier ratio

$$\frac{P_n}{P_s} = 4BL(f) \left\{ |1-H(j2\pi f)|^2 + \frac{4Q_L^2 f^2}{\nu_o^2} \right\} \qquad (2)$$

The experimental data of Fig. 6 can be interpreted in terms of Eq. (2). The noise curve (c) in the figure, obtained with the resonator removed, is a result of the first term only of the

equation, while the curve (b), which includes the resonator, contains contributions from both terms. From the noise data it can be seen that the first term is much smaller than the second and can be neglected when the cavity is present.

Eq. (2) can be used to calculate the FM noise power density L(f) of the source. With $\nu_o = 6.9 \times 10^{10}$ Hz, $Q_L = 67000$ and B = 1 Hz we find L(100) = -8dBc/Hz, L(1000) = -38dBc/Hz and L(1000) = -66dBc/Hz. These results show the expected f^{-3} dependence of the noise power density. The values obtained are in good agreement with those reported by Castro et al (10) for a 10 GHz Gunn oscillator if one scales up the noise appropriately by multiplying it by the square of the frequency ratio.

With the resonator removed the remaining noise depicted in curve (c) of the figure should be predicted from the measured L(f) and the transfer function of the local oscillator phase lock loop. When such a calculation is carried out, we find the predicted noise level to be more than 10dB lower than that observed. The excess noise actually observed is believed to be due to the internal noise of the phase lock apparatus (HP/Dymec model DY-2650A) which limits the improvement that can be obtained with the feedback loop.

Finally, we note the improvement in FM noise conversion resulting from the stabilization loop which locks the signal oscillator to the center frequency of the resonator. The total noise after stabilization is given by curve (a) in the figure. The stabilization loop gain is such that the total noise is reduced at low frequencies to a value essentially equal to the residual level of curve (c). The improvement slowly decreases with frequency in accordance with the roll off of the loop gain until at 50 KHz the level is equal to that obtained for the unstabilized cavity.

Of primary interest is the noise-to-carrier ratio at the direct output of the spectrometer, since it will limit the overall sensitivity at sufficiently high power levels. This noise

is also predicted by Eq. (1), suitably modified. Referring to the quantity, K_{dir} of that equation, we note that both terms are reduced significantly by the feedback loops as described above for the quadrature case. Of the remaining factors, the most important are the relative frequency deviation S, and the precision to which the phase angle ξ can be maintained. The deviation factor S is maintained at a small value by the cavity stabilization loop. Adjustment of the phase angle ξ is quite critical and is achieved with the use of a precision phase shifter in the 30 MHz reference circuit. In order to minimize changes in ξ as the microwave frequency is swept over the range of the gas absorption line, the path length difference between the signal oscillator and the local oscillator arms of the microwave circuit must be optimized. The path length difference is chosen to cancel the phase shift of the local oscillator resulting from the finite gain of the phase lock loop.

With the parameters S and ξ optimized, it can be seen from the above analysis that the tracking performance of the local oscillator remains as a major contributor to the source noise. Future improvements in the source noise performance of the spectrometer will require a careful examination of this component.

4. Optimization and Performance

As described in the preceeding section, the resonator stabilization scheme enables the source noise contribution to the overall spectrometer noise to be reduced to approximately -122dBc/Hz. This is an improvement of more than 20 dB over that previously obtained. At a microwave power level of -5 dBm at the input port of the resonator (-17 dBm inside the cavity) the source noise and receiver noise contributions are approximately equal. Further increases in power would therefore not result in any significant improvement in sensitivity.

However, at this power level and at the pressures employed to observe the gas resonance, a significant saturation of the absorption signal occurs. This saturation reduces the amplitude

of the signal thereby cancelling out the gains obtainable from the increased sensitivity. The power level was accordingly reduced by 10 dB to -15 dBm, at which point the saturation is reduced to about 18% as described below.

With a microwave power level of -15 dBm, measurements were made of the absorption signal from dilute samples of SO_2 in air, employing the 6(1,5) - 6(0,6) rotational transition (2) at 68972.1 MHz. The results are shown in Fig. (7). Fig. (7a) shows the signal for a concentration of 117 ppm, and Fig. (7b) shows the signal for a concentration of 5.9 ppm and the noise background obtained with zero concentration. Frequency modulation at 93 Hz was used with a modulation depth of 0.20 MHz rms. The lock in amplifier time constant was 1.0 sec and the sample pressure was 0.083 torr.

With frequency modulation, the detected signal is proportional to the derivative of the Lorentzian absorption curve. The peak-to-peak amplitudes are found from the figure to be directly proportional to the concentration to within the accuracy of the gas dilution system employed. From Fig. (7b) the minimum detectable concentration (SNR = 1) is estimated to be about 1.2 ppm. The absorption coefficient corresponding to this concentration of SO_2 is $1.7 \times 10^{-9} cm^{-1}$. With longer time constants somewhat greater sensitivity would be expected.

The observed signal amplitude can be compared to calculated values obtained from the known absorption coefficient. For 117 ppm the absorption coefficient γ_o is $1.7 \times 10^{-7} cm^{-1}$ assuming a linewidth parameter of 4.73 MHz/torr (1). From the theory described in Ref. (1), the relative change in voltage $\Delta V/V$ at the direct output of the spectrometer is given by

$$\frac{\Delta V}{V} = \frac{c \gamma_o Q_L}{2\pi \nu_o}$$

where Q_L is the resonator Q value and ν_o is the microwave transition frequency. With V = 8.05 volts, we find for ΔV, 6.35 mV. This result can be converted to the peak-to-peak value of the

derivative signal using Eq. (11) of Ref. 1 with the result that V_{pp}^{calc} = 3.31 mV. With V_{pp}^{obs} = 2.75 mV from Fig. 7 for the microwave power and sample pressure used, we find the reduction of signal due to saturation to be about 18%. This result was confirmed by measurements at lower power in which the saturation was negligible.

The effects of saturation can be reduced by increasing the gas pressure in the resonator. If the pressure is increased by a factor of three, the same amount of saturation would be expected for an increased microwave power level of 10 dB. However, the linewidth would also increase by a factor of three, with the peak height remaining the same. To recover the same amplitude for the derivative signal the modulation depth would have to be increased by a factor of three. We have found that the use of large modulation depths leads to a deterioration in the noise performance of the system. This is a result of limitations in the ability of the various feedback loops to track rapid changes in frequency of large amplitude. In effect, the microwave source frequency spends more time on the slopes of the resonator response curve with the result that more FM noise is converted to AM. Thus, the potential improvements of operation at higher pressures and source power are largely cancelled by increased modulation noise.

From the above analysis of the source noise contribution to the spectrometer, we find that future increases in performance could be expected from an improvement in the phase lock loop controlling the local oscillator. In addition to lowering the source noise, improvement of this component could result in better performance at higher operating pressures.

5. Acknowledgments

This work was performed as part of the program of the Electronics Research and Development Group of the Lawrence Berkeley Laboratory, Berkeley, California and was supported by the Department of Energy under Contract No. W-7405-ENG-48.

6. References

1. W. F. Kolbe and B. Leskovar, "Millimeter-Wave Spectrometer for Pollution Research," Lawrence Berkeley Laboratory Report, LBL-6128, February 1977.
2. B. Leskovar, and W. F. Kolbe, Detection and Measurements of Air Pollutants and Constituents by Millimeter-Wave Spectroscopy, Lawrence Berkeley Laboratory Report, LBL-7986, August 1978. Presented at the 1978 Nuclear Science Symposium, Washington, D. C., October 18-20, 1978.
3. W. F. Kolbe, H. Buscher and B. Leskovar, "Microwave Absorption Coefficients of Atmospheric Pollutants and Constituents," J. Quant. Spectrosc. Rad. Transf. 18 47 (1977).
4. H. Buscher, B. Leskovar and W. F. Kolbe, "Application of Microwave Fabry-Perot Resonators in Instrumentation for Air Pollution Research," Lawrence Berkeley Laboratory Report, LBL-4469, February 1976.
5. B. Leskovar, H. T. Buscher, and W. F. Kolbe, Piezoelectric-Tuned Microwave Cavity for Absorption Spectrometery," U. S. DOE Patent No. 4,110,686. Filed August 17, 1977, serial No. 825,503.
6. M. W. P. Strandberg, "Sensitivity of Radio Frequency Measurements in the Presence of Oscillator Noise," Rev. Sci. Instr. 43, 307 (1972).
7. B. Leskovar, D. B. Hopkins and W. F. Kolbe, "Optimal Design Criteria for Millimeter-Wave Spectrometers," Proceedings of the 5th International Microwave Conference, Hamburg, West Germany, September 1975, pp. 228-232.
8. F. M. Gardner, Phaselock Techniques, J. Wiley and Sons, New York, 1966, Chapter 4.
9. A. Blanchard, Phase-Locked Loops, Application to Coherent Receiver Design, J. Wiley and Sons, New York, 1976, Chapter 8.
10. A. A. Castro and F. P. Ziolkowski, "Generation of Millimeter-Wave Signals of High Spectral Purity," IEEE Trans. Microwave Theory Tech., Vol. MTT-24, 780 (1976).
11. G. D. Boyd and H. Kogelnik, "General Confocal Resonator Theory," Bell System Tech. J., 41, 1347 (1962).

7. Figure Captions

Fig. 1 Block diagram of microwave spectrometer.

Fig. 2a Cross-sectional view of Fabry-Perot resonator.

Fig. 2b Photographic front angle view of Fabry-Perot resonator.

Fig. 3 Piezoelectric tuning characteristics of resonator system.

Fig. 4 Dynamic tuning behavior of resonator as a function of piezoelectric drive frequency. The amplitude at low frequencies is equal to the slope of Fig. 3.

Fig. 5 Direct and quadrature output signals of spectrometer showing resonator response characteristics. Measured Q is 67000 at a center frequency of 68.97 GHz.

Fig. 6 Noise-to-carrier ratio measured at the quadrature output of spectrometer. (a) Signal oscillator locked to resonator, (b) signal oscillator free running, (c) resonator removed from system, and (d) residual noise contribution of receiver.

Fig. 7 Derivative absorption signal for SO_2 gas diluted in air. Pressure is 0.083 torr, modulation 0.20 MHz rms at 93 Hz, time constant is 1.0 sec. The detected signal is the rms component at 93 Hz of the spectrometer direct output of 8.05 volts. Fig. 7a shows the signal for 117 ppm concentration and Fig. 7b shows the signal and noise for 5.9 ppm concentration.

Table I. Noise-to-Carrier Ratio[1]

	Offset Frequency (Hz)	Phase-Locked Signal-Oscillator (dB/Hz)	Cavity Stabilized Oscillator (dB/Hz)	Receiver Noise Contribution[3] (dB/Hz)
Microwave Power Level[2] = -25 dBm	33	-98	-102	-107
	100	-99	-105	-107
	200	-99	-106	-107
	500	-100	-106	-107
	1000	-100	-106	-107
	2000	-100	-106	-107
	5000	-100	-106	-107
	10000	-101	-106	-107
Microwave Power Level[2] = -15 dBm	33	-101	-108	-115
	100	-101	-114	-116
	200	-101	-114	-116
	500	-101	-115	-116
	1000	-101	-115	-116
	2000	-101	-115	-116
	5000	-101	-115	-116
	10000	-101	-115	-116
Microwave Power Level[2] = -5 dBm	33	-101	-118	-126
	100	-101	-119	-126
	200	-101	-121	-126
	500	-101	-122	-126
	1000	-101	-122	-126
	2000	-101	-122	-126
	5000	-101	-122	-126
	10000	-101	-122	-126

[1]Noise-to-Carrier Ratio was measured in a 1 Hz bandwidth at the direct output of the phase-sensitive receiver as a function of offset frequency from the carrier for two different stabilization schemes.

[2]Microwave power level was measured at the input port of the resonator.

[3]Although the receiver noise is constant, its contribution is reduced at higher power levels because of corresponding reductions in the IF amplifier gain.

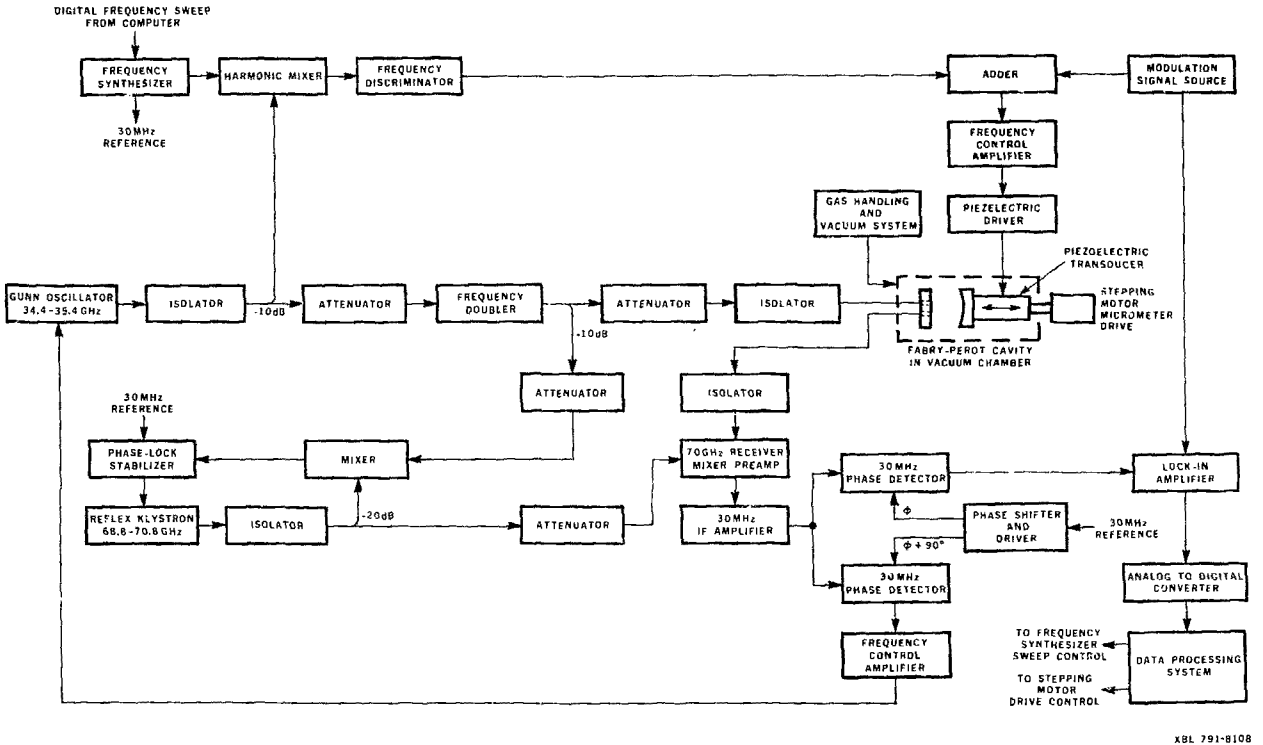
DIGITAL FREQUENCY SWEEP FROM COMPUTER
FREQUENCY SYNTHESIZER
HARMONIC MIXER
FREQUENCY DISCRIMINATOR
ADDER
MODULATION SIGNAL SOURCE
30MHz REFERENCE
FREQUENCY CONTROL AMPLIFIER
GAS HANDLING AND VACUUM SYSTEM
PIEZELECTRIC DRIVER
PIEZOELECTRIC TRANSDUCER
STEPPING MOTOR MICROMETER DRIVE
GUNN OSCILLATOR 34.4-35.4 GHz
ISOLATOR
-10dB
ATTENUATOR
FREQUENCY DOUBLER
ATTENUATOR
ISOLATOR
FABRY-PEROT CAVITY IN VACUUM CHAMBER
-10dB
ATTENUATOR
ISOLATOR
30MHz REFERENCE
PHASE-LOCK STABILIZER
MIXER
70GHz RECEIVER MIXER PREAMP
30MHz PHASE DETECTOR
LOCK-IN AMPLIFIER
REFLEX KLYSTRON 68.6-70.6GHz
ISOLATOR
-20dB
ATTENUATOR
30MHz IF AMPLIFIER
Φ
PHASE SHIFTER AND DRIVER
30MHz REFERENCE
Φ+90°
30MHz PHASE DETECTOR
ANALOG TO DIGITAL CONVERTER
FREQUENCY CONTROL AMPLIFIER
TO FREQUENCY SYNTHESIZER SWEEP CONTROL
TO STEPPING MOTOR DRIVE CONTROL
DATA PROCESSING SYSTEM
XBL 791-8108

Fig. 1

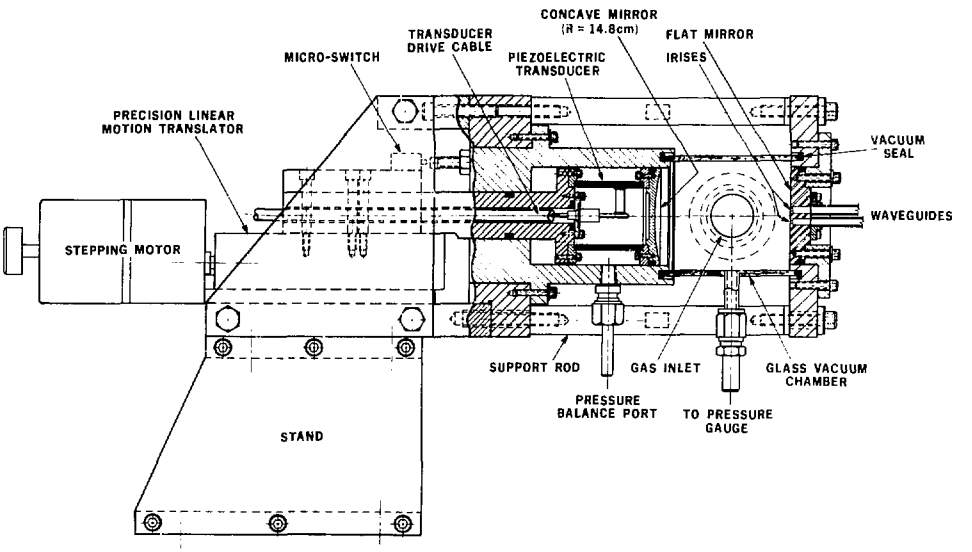

PARTIAL SIDE SECTIONAL VIEW

XBB 791-1023

Fig. 2a

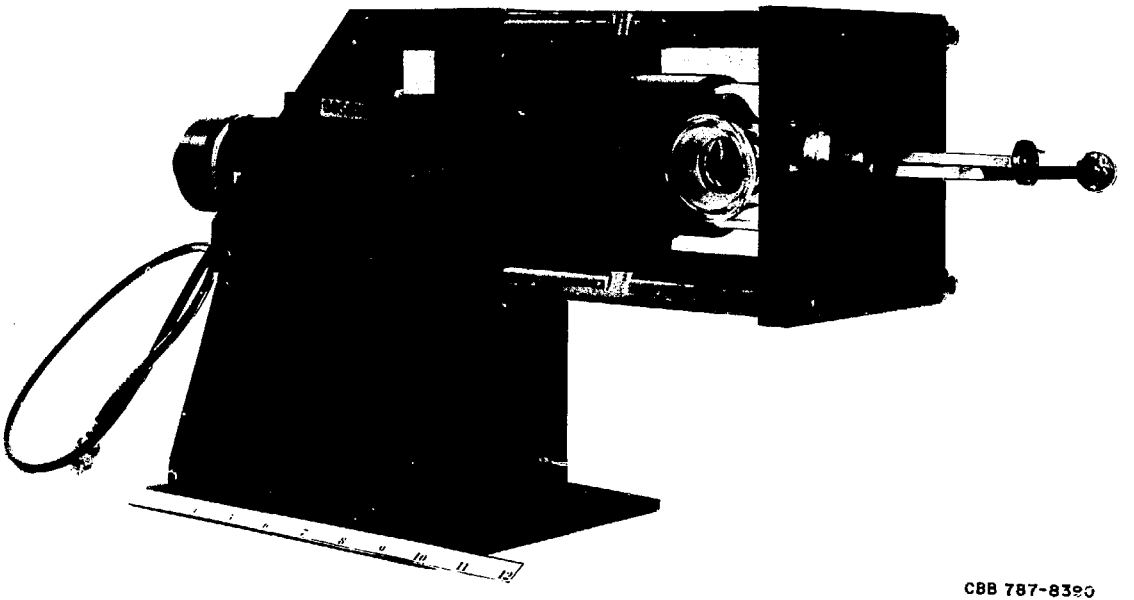

CBB 787-8390

Fig. 2b

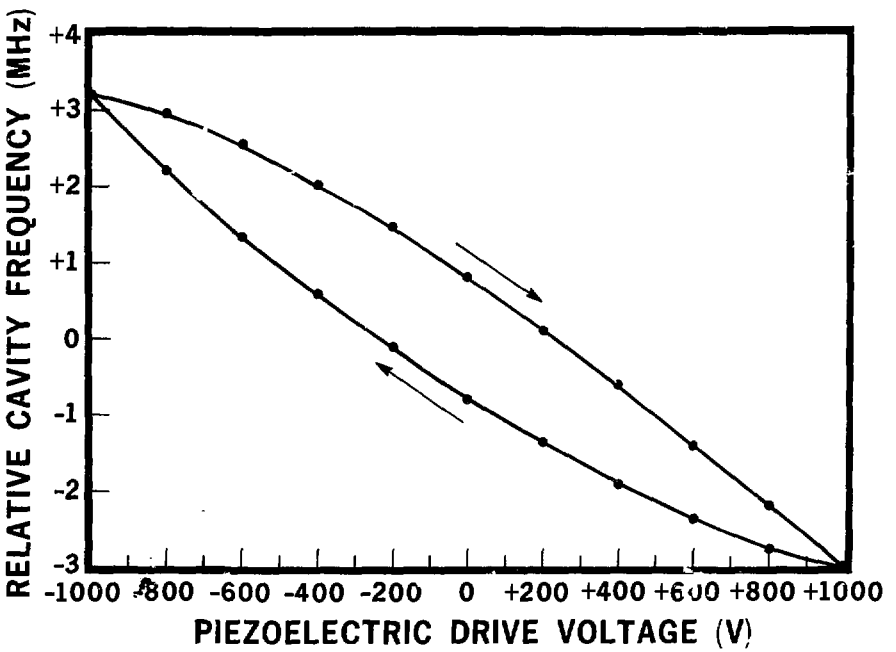
RELATIVE CAVITY FREQUENCY (MHz)
+4
+3
+2
+1
0
-1
-2
-3
-1000 -800 -600 -400 -200 0 +200 +400 +600 +800 +1000
PIEZOELECTRIC DRIVE VOLTAGE (V)
XBL 791-8110

Fig. 3

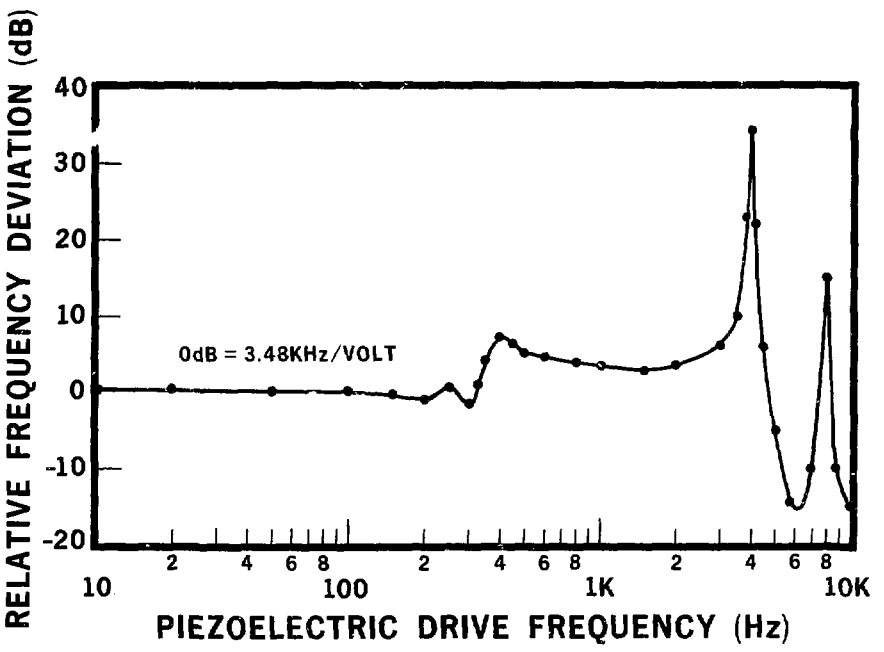
RELATIVE FREQUENCY DEVIATION (dB)
40
30
20
10
0
-10
-20
0dB = 3.48KHz/VOLT
10
2
4
6
8
100
1K
10K
PIEZOELECTRIC DRIVE FREQUENCY (Hz)
XBL 797-8111

Fig. 4

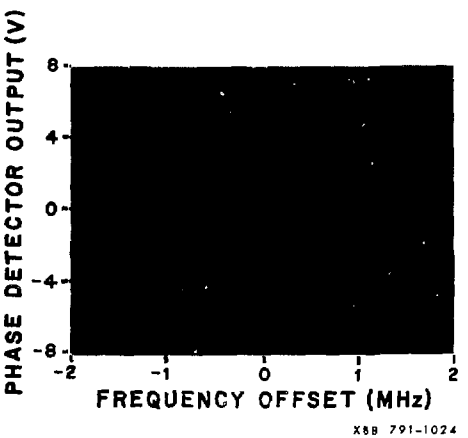
PHASE DETECTOR OUTPUT (V)
8
4
0
-4
-8
-2
-1
0
1
2
FREQUENCY OFFSET (MHz)
X8B 791-1024

Fig. 5

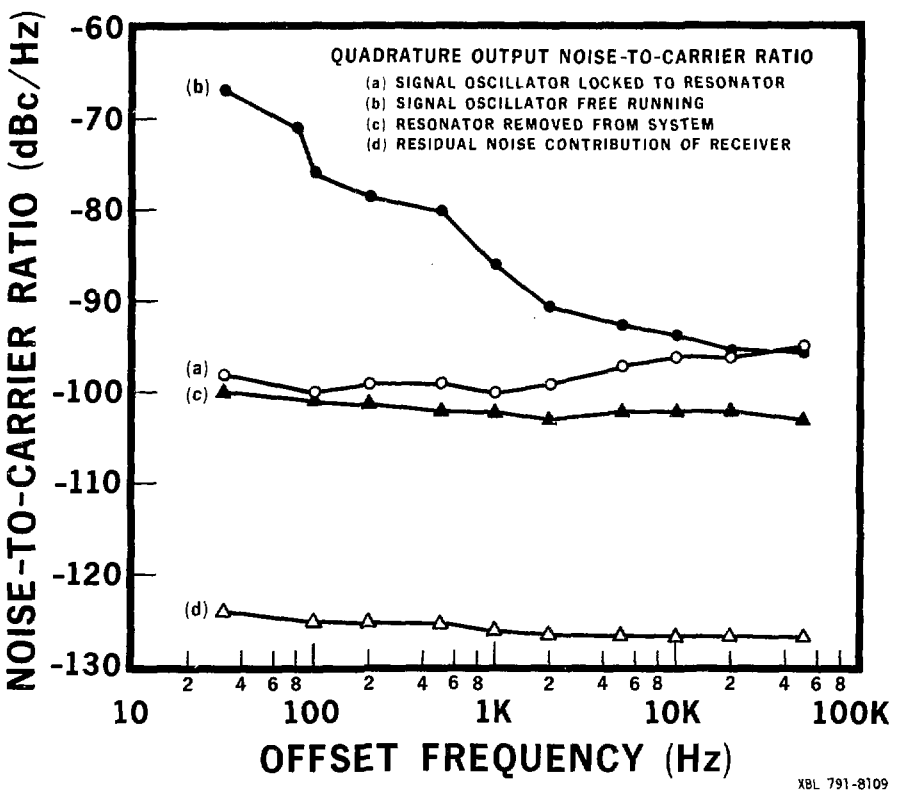
QUADRATURE OUTPUT NOISE-TO-CARRIER RATIO
(a) SIGNAL OSCILLATOR LOCKED TO RESONATOR
(b) SIGNAL OSCILLATOR FREE RUNNING
(c) RESONATOR REMOVED FROM SYSTEM
(d) RESIDUAL NOISE CONTRIBUTION OF RECEIVER
NOISE-TO-CARRIER RATIO (dBc/Hz)
-60
-70
-80
-90
-100
-110
-120
-130
(a)
(b)
(c)
(d)
2 4 6 8 2 4 6 8 2 4 6 8 2 4 6 8
10
100
1K
10K
100K
OFFSET FREQUENCY (Hz)
XBL 791-8109

Fig. 6

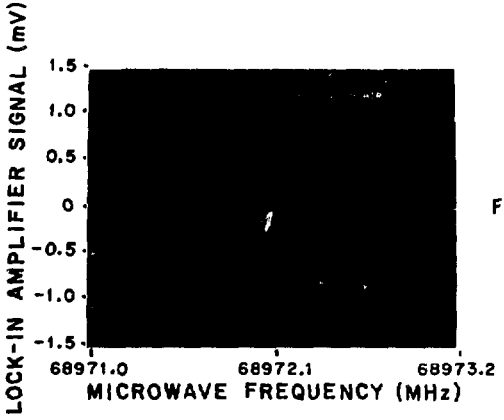

Fig. 7a

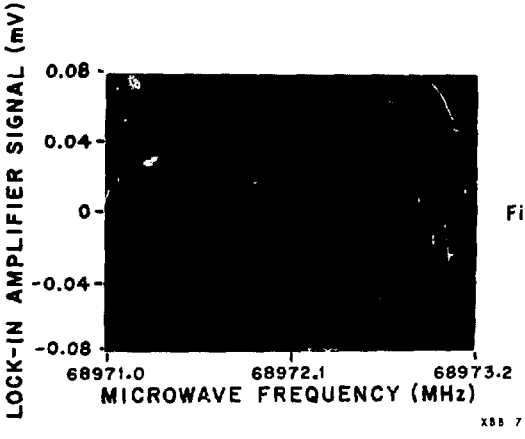

Fig. 7b

XBB 791-1022